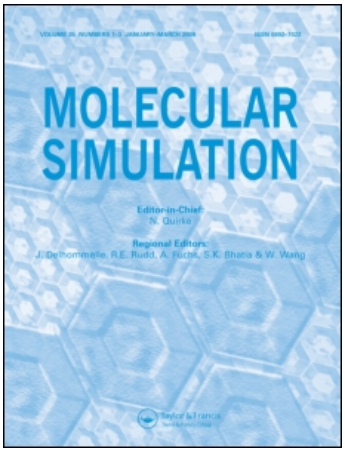

Molecular Simulation
Publication details, including instructions for authors and subscription information:
http://www.informaworld.com/smpp/title~content=t713644482

The influence of polyhydroxylated compounds on a hydrated phospholipid bilayer: a molecular dynamics study

Cristina S. Pereira[a]; Philippe H. Hünenberger[a]
[a] Laboratory of Physical Chemistry, ETH-Hönggerberg, Zürich, Switzerland

To cite this Article Pereira, Cristina S. and Hünenberger, Philippe H.(2008) 'The influence of polyhydroxylated compounds on a hydrated phospholipid bilayer: a molecular dynamics study', Molecular Simulation, 34: 4, 403 — 420
To link to this Article: DOI: 10.1080/08927020701784762
URL: http://dx.doi.org/10.1080/08927020701784762

Molecular Simulation
Vol. 34, No. 4, April 2008, 403–420

Taylor & Francis
Taylor & Francis Group

The influence of polyhydroxylated compounds on a hydrated phospholipid bilayer: a molecular dynamics study

Cristina S. Pereira and Philippe H. Hünenberger*

Laboratory of Physical Chemistry, ETH-Hönggerberg, Zürich, Switzerland

(*Received 20 July 2007; final version received 30 October 2007*)

Molecular dynamics simulations are used to investigate the interaction of the polyhydroxylated cosolutes (CSLs) methanol (MET), ethylene glycol (ETG), glycerol (GLY), glucose (GLU) and trehalose (TRH) with a hydrated phospholipid bilayer in the liquid–crystalline phase at 325 K. The comparison is performed at constant effective concentration of CSL hydroxyl groups. The results (along with available experimental data) lead to the formulation of two distinct mechanisms for the interaction of polyhydroxylated compounds with lipid bilayers. The alcohol-like mechanism (active for MET and ETG) involves preferential affinity of the CSL (compared to water) for the superficial region of the bilayer interior, and is driven by the hydrophobic effect. It results in a lateral expansion of the membrane, a disorder increase within the bilayer, and a partial substitution of water by CSL molecules at the hydrogen-bonding sites provided by the membrane (predominantly at the level of the ester groups). The sugar-like mechanism (active for GLU and TRH) involves preferential affinity of the CSL (compared to water) for the bilayer surface (formation of a coating layer), and is driven by entropic effects. It results in the absence of lateral expansion and change in disorder within the bilayer, and in a partial substitution of water by CSL molecules (predominantly at the level of the phosphate groups). It also involves the bridging of lipid molecules via hydrogen-bonded CSL molecules, a phenomenon that may have implications in the context of membrane stabilisation by sugars. Hydrogen bonding itself is not viewed as a driving force for these two mechanisms, which only involve the (partial) substitution of water–lipid by CSL–lipid hydrogen bonds (the sum of the two remaining essentially constant, irrespective of the nature and concentration of the CSL).

Keywords: trehalose; glucose; polyols; DPPC; molecular dynamics

1. Introduction

The cell membrane constitutes the first site of interaction of a cell with its extracellular environment. As a consequence, it assumes a number of key roles in the cellular function [1,2] such as confinement, protection, selective permeation of substances, preservation of the cell potential and cell signaling (through specific embedded proteins and exposed oligosaccharides). In animal cells, the membrane alone establishes a separation between the interior and the extracellular medium, whereas in fungi, bacteria and plants, an additional cell wall forms the outermost boundary. However, this wall functions mostly as a mechanical support rather than as an additional selective boundary [1].

Since biomembranes are the first component of the cell to interact with any external solute, the presence of cosolutes (CSL) or cosolvents (both further collectively referred to as CSLs for simplicity) at sufficiently high concentrations in the extracellular (and possibly also intracellular) medium may alter their physicochemical properties. This may in turn affect the functioning of intrinsic membrane proteins such as ion and water channels [3,4], or the resistance of the cell to potentially damaging conditions [5–7]. For this reason, the modulation of membrane properties by CSLs, and in particular by small mono- and polyhydroxylated compounds (both further collectively referred to as polyhydroxylated compounds for simplicity), is involved in several processes of high biological, technological and medicinal relevance. For example, sugars (prominently trehalose (TRH) and sucrose) play a central role in the ability of certain organisms to survive extreme conditions of dehydration, temperature, pressure, oxygen deprivation or salt concentration [5–7]. Alcohols and other small molecules are used as anaesthetics agents [8–10]. Glycerol (GLY) and ethylene glycol (ETG) are commonly used as cryoprotective agents to minimise cellular damage in freezing technologies [11,12]. All these phenomena appear to involve, among other effects, a modulation of the properties of the cell membrane by the CSL molecules [3–12].

The mechanisms whereby, sugars stabilise biomembranes under harsh conditions remain nowadays matter of debate. In the (experimentally best documented) case of dehydration resistance, three main hypotheses have been put forward. The water-replacement hypothesis suggests that sugars can substitute water molecules, in particular by forming hydrogen bonds (H-bonds), around the polar and charged groups present at the surface of phospholipid membranes, thereby maintaining the spacing between the

*Corresponding author. Email: phil@igc.phys.chem.ethz.ch

ISSN 0892-7022 print/ISSN 1029-0435 online

DOI: 10.1080/08927020701784762
http://www.informaworld.com

headgroups and preserving the membrane in the liquid–crystalline phase throughout the dehydration–rehydration cycle. In contrast, the water-entrapment hypothesis (mainly documented in the context of protein stabilisation) proposes that sugars concentrate residual water molecules close to the biomolecular surface, thereby preserving to a large extent its solvation and native properties [14]. Finally, the vitrification hypothesis suggests that sugars found in anhydrobiotic systems (known to be good vitrifying agents) protect biomembranes through the formation of amorphous glasses, thereby reducing structural fluctuations and preventing mechanical disruption [15]. In the last few years, a consensus has emerged that these mechanisms are not necessarily mutually exclusive [5,6,16,17]. In particular, it is likely that vitrification and a direct H-bonding interaction of the sugar molecules with the lipid headgroups are simultaneously required to achieve bioprotection.

The suggestion that the physiological effects of alcohols and other anaesthetics are (at least in part) due to the modulation of membrane properties is supported by the apparent lack of specific receptor sites for these molecules in the cell [18]. A non-specific interaction is also consistent, for example, with the characteristics of ethanol intoxication, where a relatively high concentration is required to produce a response (above which the response is enhanced upon further increasing the concentration). However, the exact mode of action of alcohols and other anaesthetic agents, as well as the hypotheses invoking lipids as the prime target in these processes, remain matter of debate [18,19]. The interaction of alcohols with lipid membranes presents a peculiar characteristic, the so-called 'biphasic' effect [20]. Depending on the concentration range, short-chained aliphatic alcohols have an opposite influence on the main gel to liquid–crystalline phase transition temperature (T_m) of membranes. At low concentrations, T_m decreases with increasing alcohol concentration, whereas at high concentrations, the opposite trend is observed. The concentration where this reversal takes place for a given alcohol strongly depends on the length of the lipid hydrocarbon chains [20]. The biphasic effect was explained by the alcohol-induced formation of an unusual interdigitated gel phase, where lipid molecules from the opposing monolayers interpenetrate [21]. At low alcohol concentrations, the usual lamellar gel phase is destabilised over the liquid crystalline one (presumably through the intercalation of alcohol molecules between the lipid headgroups and the concomitant increase in the area per lipid; see below) leading to the observed T_m decrease. At high concentrations the interdigitated phase can be formed (its stability relative to the liquid crystalline phase increasing with the alcohol concentration), resulting in the observed T_m increase. The occurrence of an interdigitated phase at high alcohol concentrations can be interpreted as an extreme consequence of the same effect that induces the T_m decrease at lower concentrations, namely the intercalation of the alcohol molecules between the lipid headgroups [22–25]. This results in an increase of the effective headgroup volume, inducing a lateral expansion in the interfacial region [26–28]. When this expansion is important enough, the (energetically unfavourable) void spaces within the bilayer interior can be removed through interdigitation of the lipid tails [21–31]. All short-chain aliphatic alcohols (methanol (MET) through heptanol) induce interdigitation at sufficiently high concentrations [26,30,31]. However, longer chain alcohols may induce a different response, presumably because their aliphatic chains are also able to intercalate between the lipid tails [32]. In line with the general tendency of alcohols to increase the headgroup spacing, an increase in the disorder (decrease in the order parameters) of the lipid hydrocarbon tails is observed when alcohols are added to phospholipid bilayers in the liquid crystalline phase ([23–25]; provided that the system does not undergo transition to the interdigitated gel phase). This disorder increase is caused by a reduction of the packing constraints imposed to the lipid tails.

Similarly to short-chain aliphatic alcohols, GLY and ETG can induce (at sufficiently high concentrations) the formation of interdigitated phases in phospholipid bilayers [33–36]. Multilamellar liposomes can be formed in pure GLY with similar properties (spacing between bilayers, main transition temperatures, heat capacities and enthalpies) to those formed in pure water [33]. Such liposomes can also be formed in pure ETG [33]. ETG in aqueous solution has also been shown to present a biphasic effect [36] and to promote an increase in the disorder of the lipid tails [37,38] for bilayers in the liquid crystalline phase. A number of studies have suggested that GLY interacts directly (through H-bonds) with the lipid headgroups [39,40]. However, a recent calorimetric investigation has concluded that GLY is preferentially excluded from the membrane-water interface [41], in apparent disagreement with the previous experimental studies.

In spite of numerous investigations, experimental approaches alone have not been able to provide a complete understanding of the molecular mechanisms underlying the modulation of bilayer properties by polyhydroxylated CSLs. For this reason, experimental approaches can be very valuably complemented by atomistic computer simulations, that are able to provide information on a temporal (femtosecond) and spatial (atomic) resolution inaccessible to most experimental methods.

In the past years, several computational studies investigating the properties of pure hydrated membranes from an atomistic perspective have contributed to establish explicit-solvent molecular dynamics (MD) simulation as one of the most powerful techniques for the investigation of the structural, dynamical and thermodynamical properties of these systems [42–44]. These studies evaluate the

properties of model membranes with an impressive level of details, and an ever increasing degree of reliability (as established by comparison with available experimental observables). Although, most MD studies to date addressed the properties of pure hydrated membranes (see [45,46] for recent reviews), there have been a few computational investigations focusing on the influence of CSLs on the properties of lipid bilayers. These recent studies have been concerned with the effect of small CSL molecules like dimethylsulfoxide [47], anaesthetics [48–51], sugars [52–58] and aliphatic alcohols [59–64]. To our knowledge, no such study has investigated the effect of simple polyols (e.g. ETG and GLY). In general, the results of independent investigations (using different force fields and simulation protocols for similar systems) present a good qualitative agreement. The key results of these studies concerning polyhydroxylated compounds (focusing on sugars and short-chained aliphatic alcohols) are summarised below. For the ease of comparison, CSL concentrations are reported in molal (m) units (i.e. mol CSL per kg solvent).

Simulation studies on the interaction of sugars with membranes [52–58] have been primarily motivated by the lack of understanding and controversial hypotheses [5,6,13–17] concerning the molecular mechanisms involved in biostructure preservation by sugars [5–7]. These studies have shown that under normal conditions of temperature and pressure, sugars tend to promote a moderate increase in the area per lipid and in the extent of disorder within the bilayer. In addition, these molecules have been observed to establish H-bonds with the lipid headgroups, partially replacing water molecules at the surface of hydrated phospholipid bilayers [52–58]. The comparison of simulations involving different sugar CSLs has not revealed striking differences in their influence on the membrane properties [52,57]. Note, however, that the imposition of stress to the bilayer (e.g. elevated temperature or negative lateral pressure) has a strong influence on the way sugar molecules interact with the lipid headgroups (increase in the number of sugar–lipid H-bonds and in the degree of bridging of the lipids via H-bonded sugar molecules; [53,57,58]).

Simulation studies on the interaction of aliphatic alcohols with lipid membranes have shown that the shortest-chain alcohols (MET, ethanol and propanol) increase the area per lipid, and that this increase is essentially proportional to the alcohol concentration [59–64], in agreement with experiment [28]. However, a slight decrease in the area per lipid was observed for butanol [64], in disagreement with experiment [28]. With respect to the effect of MET on the order parameters of the lipid-tail carbon atoms, simulations have led to apparently contradictory results. The study of Pinisetty et al. [61], performed at relatively high MET concentration (11.3 mol%, i.e. 6.3 m) for dipalmitoylphosphatidylcholine (DPPC) and palmitoyloleoylphosphatidylcholine (POPC) bilayers, reported a significant decrease in the order parameters compared to the pure hydrated systems (concomitant with a substantial increase of about 15% in the area per lipid). In contrast, the study of Patra et al. [62], performed at a lower MET concentration (1 mol%, i.e. 0.6 m) for the same type of lipid bilayers, reported a slight increase in the order parameters (concomitant with a more limited increase of about 6% in the area per lipid), the same trend being observed for ethanol (at the same concentration). The available experimental data for dimyristoylphosphatidylcholine (DMPC) and POPC bilayers in the presence of ethanol ([23]; molar ratio lipid:ethanol:water 1:2:4 and 1:1:10, i.e. 27.8 and 5.6 m, respectively) and for POPC with ethanol ([24]; molar ratio lipid:ethanol:water 1:1:10, i.e. 5.6 m) shows a decrease in the order parameters, in agreement with the trend observed for MET in the first simulation study [61]. The apparent contradiction between simulation and experimental results for ethanol ([62] vs. [24]) is rationalised by the authors [62] as being a consequence of the different concentration regimes and hydration levels considered. The same argument may apply to the differences observed between the two simulation studies for MET ([62] vs. [61]). A decrease in the order parameters, the magnitude of which increased with the alcohol concentration, was also observed in other simulation studies for MET (3 and 5 wt%, i.e. 1.0 and 1.6 m [60]) and ethanol (1 wt%, i.e. 0.2 m; [60]), as well as for ethanol (1.9 and 10.6 mol%, i.e. 1.1 and 6.6 m [64]) and propanol (0.2 and 1.8 mol%, i.e. 0.1 and 1.0 m; [64]). Direct interactions between the CSL molecules and the lipids have been observed in the form of H-bonds between the alcohol hydroxyl groups and both the phosphate and ester groups of the lipids [63,64], in agreement with experimental observations [24,26]. One of these studies suggested that MET and ethanol differ dramatically in their ability to interact with the lipids and to penetrate into the bilayer [62]. In the low concentration regime investigated (1 mol%, i.e. 0.6 m), ethanol was found to extensively bind to the lipid headgroups through H-bonds, whereas, no single H-bond between MET and lipid molecules could be detected. Moreover, ethanol was able to penetrate (and even cross) the bilayer, whereas no single crossing event was observed for MET. These differences were interpreted as resulting from the higher polarity of MET compared to ethanol, disfavouring its penetration in the (highly hydrophobic) bilayer interior and hindering the establishment of H-bonds with the lipid headgroups ([62]; due to the stronger hydration of the methanol molecules). However, these observation should be taken with some caution, since this same study reported an increase in the order parameters upon addition of either of the two alcohols, in contradiction with experiments (in the more concentrated regime; [23,24]) and independent simulations results (in a similar concentration regime; [60,64]).

In the present work, explicit-solvent MD simulations are used to investigate and compare at the molecular level the influence of the polyhydroxylated CSLs MET, ETG, GLY, β-D-glucopyranose (GLU) and α,α- trehalose (TRH), see Figure 1, on the structure, stability and dynamics of a hydrated DPPC bilayer in the liquid–crystalline phase. A total of six independent 15 ns simulations involving the pure bilayer (no CSL) or the bilayer in the presence of the different CSLs are performed at 325 K, so as to provide a better understanding of CSL–lipid interactions, their variation along the series of compounds and their influence on the bilayer properties. The CSL concentrations are systematically decreased from MET to TRH, so as to (approximately) keep the same effective concentration of CSL hydroxyl groups in the different systems. This permits to investigate specifically the effect of the configurational (geometrical and stereochemical) restrictions imposed by a given molecular framework on the capacity of the CSL hydroxyl groups to interact with the lipid molecules. Note that, although, MD simulations of lipid bilayers in the presence of MET [60–62], GLU [57] and TRH [52–58] have been previously reported, the present work constitutes (to our knowledge) the first simulation study on the influence of ETG and GLY on membranes.

2. Methods

2.1. Molecular dynamics simulations

All MD simulations were carried out using the GROMOS96 program [65] together with the GROMOS 45A4 [66] force field, including recently re-optimised parameter sets for lipids [67] and carbohydrates [66,68,69], and the SPC water model [70]. GROMOS-compatible models were used for MET [65], ETG [71] and GLY (Geerke, personal communication; the corresponding parameters are provided as supplementary material). Newton's equations of motion were integrated based on the leap-frog algorithm [72] using a 2 fs time step. The SHAKE procedure [73] was applied to constrain all bonds lengths with a relative geometric tolerance of 10^{-4}. The simulations were carried out in the isothermal–isobaric (NPT) ensemble. The temperature was maintained at an average value of 325 K by coupling separately the solute and solvent degrees of freedom to a heat bath [74], with a relaxation time of 0.1 ps. The pressure was maintained at an average value of 1 atm by coupling the atomic coordinates and box dimensions to a pressure bath [74] via anisotropic coordinate scaling, with a relaxation time of 0.5 ps and an isothermal compressibility of 0.46×10^3 $(\mathrm{kJ\,mol^{-1}\,nm^{-3}})^{-1}$. Removal of the centre of mass motion was performed every 100 ps. Non-bonded interactions were handled using a twin-range cutoff scheme [75]. Within a short-range cutoff radius of 0.8 nm, the interactions were evaluated every time step based on a pairlist updated every five steps. The intermediate-range interactions up to a long-range cutoff radius of 1.4 nm were evaluated simultaneously with each pairlist update, and assumed constant in between. To account for the mean effect of electrostatic interactions beyond the long-range cutoff radius, a reaction-field correction [76] was applied using a relative dielectric permittivity of 54 for the solvent, as appropriate for the SPC water model [70]. Trajectory frames were saved to file every 1 ps for analysis.

2.2. Molecular systems

A hydrated bilayer of 2×64 DPPC molecules was simulated in the absence or in the presence of the different

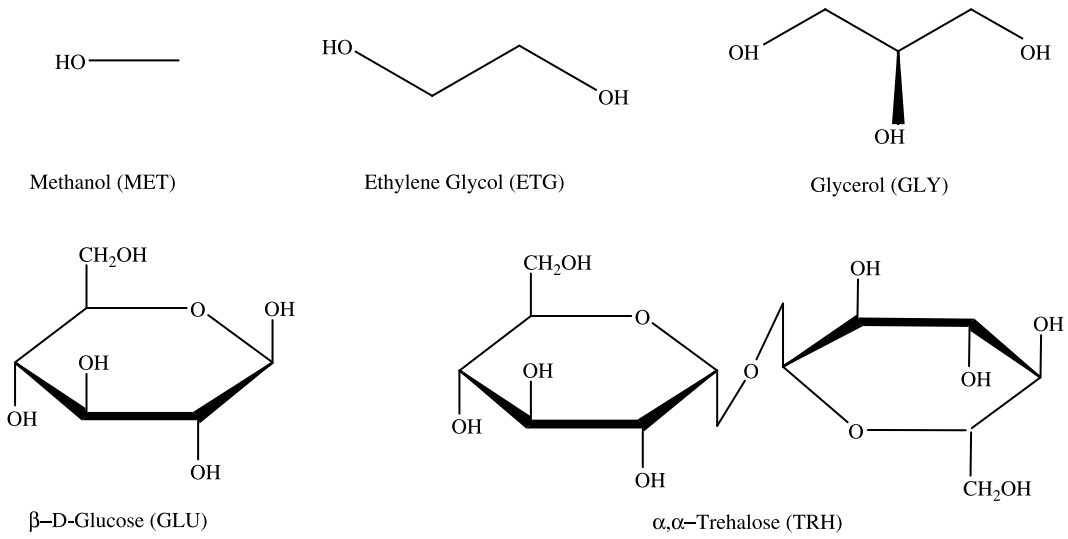

Figure 1. Schematic drawings of the CSLs considered in the present study.

CSLs at 325 K and 1 atm. A total of six independent MD simulations were carried out involving the DPPC bilayer in an aqueous solution containing either: (i) no CSL (3655 water molecules; control simulation); (ii) 1024 MET molecules; (iii) 512 ETG molecules; (iv) 384 GLY molecules; (v) 256 GLU molecules; (vi) 128 TRH molecules. The number of water molecules for the systems containing CSLs was 3339 in all cases. A summary of the simulated systems and solution concentrations is provided in Table 1.

The relative amounts of the different CSLs were selected to (approximately) keep the same effective concentration of CSL hydroxyl groups in the different systems. This was done, so as to specifically investigate the effect of the configurational (geometrical and stereochemical) restrictions imposed by a given molecular framework (Figure 1) on the capacity of the CSL hydroxyl groups to interact with the lipid molecules. The ring oxygen atoms in GLU and TRH, as well as the glycosidic oxygen atom in TRH, do not represent significant sites for interaction with the lipids since they can only function as H-bond acceptors (just as the lipid phosphate and ester groups). Note that the effective concentration of CSL hydroxyl groups is 17.0 m for the MET, ETG and TRH systems. It is slightly higher for the GLY (19.1 m) and GLU (21.3 m) systems.

A DPPC bilayer at full hydration (3655 water molecules, i.e. 28–29 molecules per lipid) in the liquid–crystalline phase, previously equilibrated during a 2.5 ns MD simulation at 325 K, was used to initiate the production run of the simulation without CSL. The box dimensions were $5.8 \times 6.2 \times 7.3\,\mathrm{nm}^3$, where the last dimension (z-axis) refers to the bilayer normal. In the simulations including CSLs, the water molecules were deleted and the corresponding number of CSL molecules (Table 1) were uniformly distributed over the box, maintaining a distance of at least 0.5 nm between any atom of a CSL molecule and any other atom within the system (lipid bilayer and other CSL molecules). The systems were then resolvated using 3339 water molecules (i.e. 26–27 molecules per lipid), imposing a minimum distance of 0.28 nm between water oxygen atoms and any solute atom. This was followed by a thorough equilibration procedure (involving in particular the relaxation of the CSL–water mixture by a 5 ns simulation at 500 K with positional restraints on the lipid molecules) as described in details elsewhere [53]. The initial box dimensions (after equilibration) were approximately the same for all systems containing CSLs: MET ($5.9 \times 6.4 \times 8.6\,\mathrm{nm}^3$), ETG ($6.0 \times 6.4 \times 8.4\,\mathrm{nm}^3$), GLY ($5.8 \times 6.3 \times 8.5\,\mathrm{nm}^3$), GLU ($5.8 \times 6.3 \times 8.5\,\mathrm{nm}^3$) and TRH ($5.8 \times 6.2 \times 8.5\,\mathrm{nm}^3$). After equilibration, all six production runs were carried out for a total duration of 15 ns.

Table 1. Summary of the simulated systems involving CSLs.

CSL	N° of OH groups	N° of molecules	Molality (m)	mol%	wt%
MET	1	1024	17.02 (17.0)	23.5	35.4
ETG	2	512	8.50 (17.0)	13.3	34.5
GLY	3	384	6.38 (19.1)	10.3	37.0
GLU	5	256	4.25 (21.3)	7.1	43.3
TRH	8	128	2.13 (17.0)	3.7	42.1

Note: Number of hydroxyl (OH) groups per CSL molecule (Figure 1), total number of CSL molecules in the simulation box, and corresponding concentrations in the solution surrounding the bilayer, defined as: molality (mol CSL per kg solvent); mol percentage (mol%; mol CSL per mol CSL and mol solvent); weight percentage (wt% weight CSL per weight solution). The number of DPPC molecules is 128 for systems. The number of water molecules is 3339 for systems containing CSL or 3655 for the system in the absence of CSL. The effective molality in terms of CSL hydroxyl groups is also indicated between parentheses.

2.3. *Analyses*

The trajectories were analysed in terms of the area per lipid for the DPPC molecules; the deuterium order parameters (S_{CD}) for the two acyl chains of DPPC (sn-1 and sn-2); the normalised density profiles for specific reference atoms of DPPC (phosphorus atom, nitrogen atom, and glycerol CH1 united atom), MET (oxygen atom), ETG (oxygen atom), GLY (oxygen atom of the central hydroxyl group), GLU (lactol oxygen atom), TRH (glycosidic oxygen atom), and water (oxygen atom) along the bilayer normal (z-axis of the simulation box); the lateral (xy-plane of the simulation box) diffusion coefficients (D_{xy}) for DPPC, MET, ETG, GLY, GLU, TRH and water molecules (same reference atoms for water and CSLs, central glycerol CH1 united atom for DPPC); the H-bonds, classified according to pairs of species present in the simulated systems; the degree of bridging of the lipids via H-bonded CSL molecules. The criterion used to define a H-bond was a hydrogen-acceptor distance shorter than 0.25 nm and a donor-hydrogen-acceptor angle larger than 135°. All the oxygen atoms of DPPC and CSLs were considered as H-bond acceptors, and all the hydroxyl groups of the CSLs as H-bond donors. A more detailed description of the analysis procedure can be found elsewhere [53].

3. Results

The time evolution of the area per lipid of the bilayer is shown in Figure 2 for the six simulations. In the absence of CSL, the area remains stable at about $0.56\,\mathrm{nm}^2$ (average over the final 6 ns of the simulation). This value is in the expected range for a fully-hydrated DPPC membrane in the liquid–crystalline phase simulated using the present force-field and simulation conditions [67,77], although, it is on the low side compared to the best experimental estimate of $0.64\,\mathrm{nm}^2$ [78]. However, the difference may arise (at least in part) from the microscopic size and

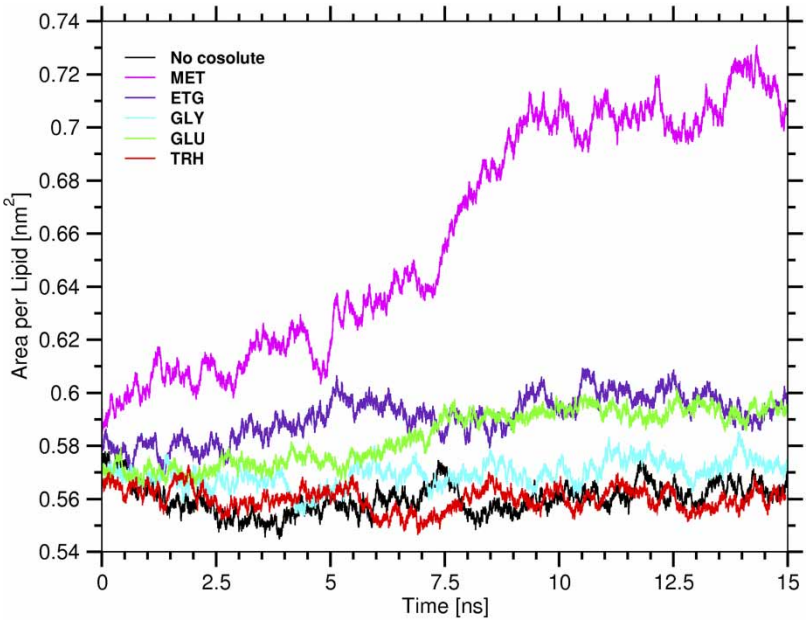

Figure 2. Area per lipid as a function of time for the six simulations of a DPPC bilayer in the absence or in the presence of different CSLs (Figure 1 and Table 1) at 325 K.

artificial periodicity of the simulated membrane patch which, unlike its experimental counterpart, cannot undergo undulations over a significant lengthscale [77]. The area per lipid is essentially unaltered in the presence of TRH (average value of 0.56 nm^2 over the final 6 ns), while a very slight increase (2%; average value of 0.57 nm^2 over the final 6 ns) is observed for the system containing GLY. In the presence of ETG and GLU, the

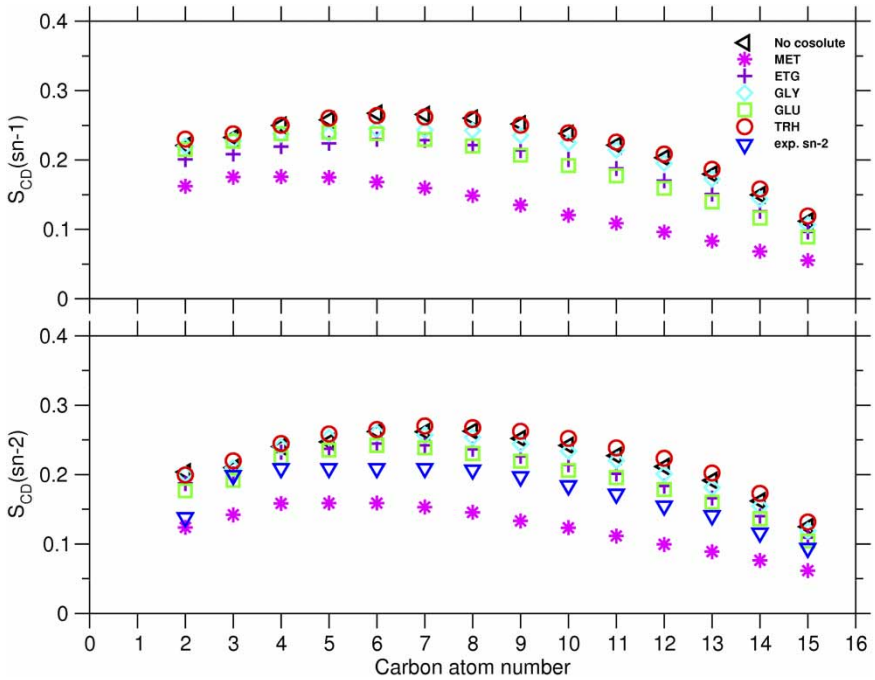

Figure 3. Deuterium order parameters (S_{CD}) as a function of the carbon atom number along the sn-1 (top) and sn-2 (bottom) chains, calculated for the six simulations of a DPPC bilayer in the absence or in the presence of the different CSLs (Figure 1 and Table 1) at 325 K. Experimental values for the sn-2 chain at 325 K [47] are also given for comparison. The values are averaged over the 128 DPPC molecules and over the final 6 ns of the simulations.

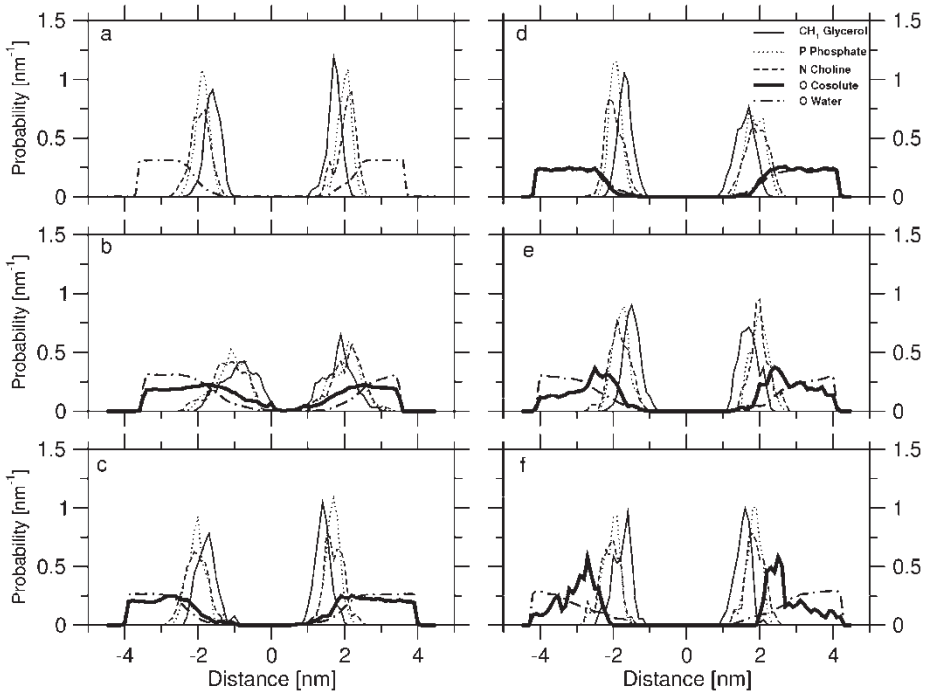

Figure 4. Normalised density profiles for specific reference atoms of the DPPC, CSL and water molecules along the bilayer normal (z-axis), calculated for the six simulations of a DPPC bilayer in pure water (a), or in the presence of the different CSLs (Figure 1 and Table 1), namely MET (b), ETG (c), GLY (d), GLU (e) or TRH (f) at 325 K. The profiles correspond to averages over the final 0.25 ns of the simulations and are displayed for a single copy of the computational box centred on the bilayer midplane (minimum image convention).

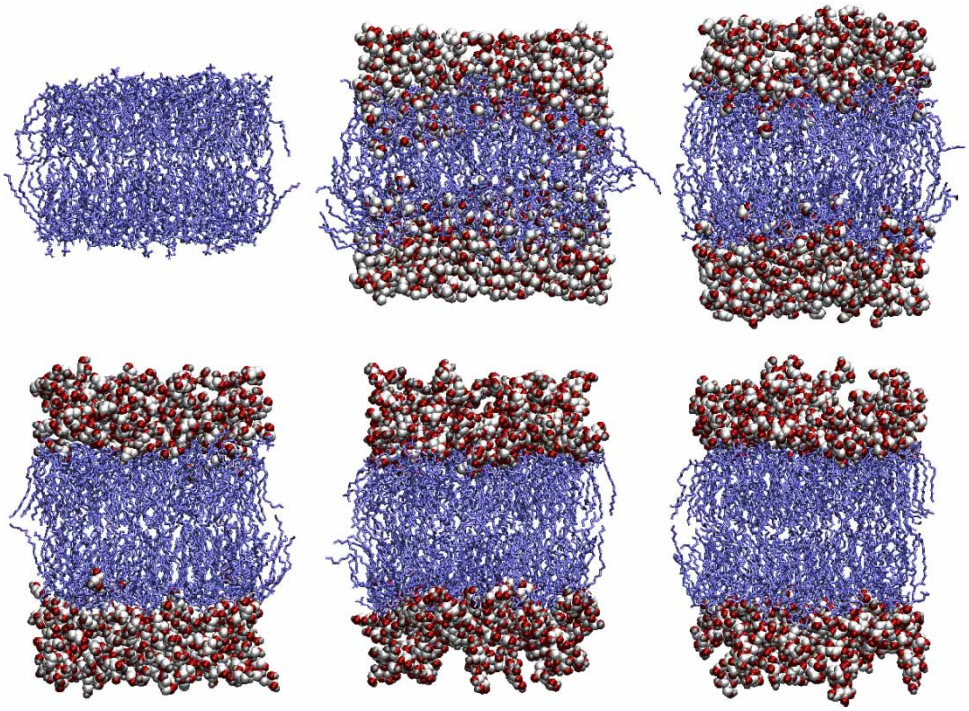

Figure 5. Final configurations (15 ns) of the simulations of a DPPC bilayer in pure water (top left) or in the presence of the different CSLs (Figure 1 and Table 1) at 325 K, namely MET (top centre); ETG (top right); GLY (bottom left); GLU (bottom centre); TRH (bottom right). Water molecules have been removed for clarity. All CSL molecules are represented using a spacefill model where carbon atoms are white, oxygen atoms red and hydrogen atoms grey. DPPC molecules are represented in blue using a stick model.

Table 2. Lateral diffusion coefficients (D_{xy}) for DPPC, CSL and water molecules during the six simulations of a DPPC bilayer in the absence or in the presence of different CSL (Figure 1 and Table 1) at 325 K.

	DPPC D_{xy} ($10^{-5}\,cm^2\,s^{-1}$)	CSL D_{xy} ($10^{-5}\,cm^2\,s^{-1}$)	Water D_{xy} ($10^{-5}\,cm^2\,s^{-1}$)
No CSL	0.078	–	4.80
MET	0.042	2.24	4.21
ETG	0.180	1.52	3.74
GLY	0.084	1.06	3.26
GLU	0.022	0.24	2.63
TRH	0.012	0.08	2.66

Note: The values are averaged over all molecules of a given kind and calculated over the final 6 ns of the simulations.

area per lipid is noticeably increased compared to the simulation without any CSL (by 7 and 5%, respectively; average values of 0.60 and 0.59 nm^2, respectively, over the final 6 ns). Finally, the largest effect is observed for the system containing MET, where a large increase in the area per lipid occurs along the simulation (27% increase; average value of 0.71 nm^2 over the final 6 ns). The observed lateral expansion of the membrane in the presence of polyhydroxylated CSLs (except GLY and TRH) is in good qualitative agreement with the results of experimental studies on DPPC bilayers (as well as bilayers involving other lipids) in the presence of aliphatic alcohols [2,25,27,28] and sugars [13,17,79,80]. An increase in the area per lipid in the presence of MET was also found in recent MD simulation studies on the influence of this alcohol on DPPC and DOPC lipid bilayers [61,62]. However, the increase observed for DPPC in the present study (27%) is more significant than those reported in the two quoted studies (15% for [61] and 6% for [62]), which is probably due to the higher MET concentration probed here (17.0 m vs. 6.3 m for [60] and 0.6 m for [62]). The usual explanation for the observed increase in the area per lipid caused by polyhydroxylated CSLs is that small molecules rich in hydroxyl groups may intercalate between the lipid headgroups, thereby increasing the spacing between the lipid chains. The results of Figure 2 further suggest that this intercalation propensity (at constant effective hydroxyl group concentration) is largest for the smallest CSL (MET) and essentially negligible for the largest one (TRH). However, the ranking of the different compounds, MET $\gg$ ETG $\sim$ GLU $\gg$ GLY $>$ TRH, is not systematic in terms of molecular size.

The analysis of the order parameters (S_{CD}) shows how the ordering of the DPPC sn-1 and sn-2 acyl chains is affected by the presence of the different CSLs (Figure 3). Although, the S_{CD} values for the sn-2 chain in the absence of CSL are somewhat overestimated compared to available experimental data [81], a known feature of the lipid force field employed in the present simulations [67], this is not expected to significantly affect the qualitative trends observed along the CSL series. The effect of the different CSLs on the two lipid chains, sn-1 and sn-2, is essentially the same. The order parameters are not significantly affected by the presence of TRH (or are slightly increased; tail region of the sn-2 chain). The inclusion of all the other CSLs promotes a decrease in the values. The decrease is moderate for GLY, somewhat more pronounced for ETG and GLU, and very large for MET. The latter observation for MET indicates a high degree of disorder within the bilayer and, indirectly, an enhanced conformational flexibility and mobility of the lipid chains. The differences in the order parameters caused by the presence of the different CSLs are most pronounced and systematic in the tail regions of both chains (carbon atoms C7—C16). The observed trends clearly parallel those reported for the area per lipid (Figure 2), i.e. a lateral expansion of the bilayer reduces the packing constraints imposed to the acyl chains, allowing for motions of larger amplitudes which promote an increase in disorder. The results obtained for TRH and ETG agree qualitatively with experimental studies evidencing a limited ordering effect in the hydrophobic interior of a POPC membrane upon inclusion of TRH [38], and a disordering effect in both the headgroup and tail regions upon inclusion of ETG [37,38]. For MET, the presently observed decrease in the order parameters (at 17.0 m concentration) is in line with the MD results of Pinisetty et al. in the high concentration regime (6.3 m; [61]), as well as with experimental results on closely related systems (ethanol; DMPC bilayer, 5.55 and 27.8 m solutions [23] and POPC bilayer, 6.6 m solution [24]). In contrast, the MD simulation results of Patra et al. for MET suggested a slight increase in the order parameters in the lower concentration regime (0.6 m; [62]).

The mobility of DPPC, CSL and water molecules in the different systems was analysed by calculating the corresponding lateral (two-dimensional) diffusion coefficients D_{xy} (Table 2). The value of D_{xy} for water in the absence of sugar ($4.80 \times 10^{-5}\,cm^2\,s^{-1}$) is somewhat higher than the experimental value $D = 3.47 \times 10^{-5}\,cm^2\,s^{-1}$ for the (three-dimensional) self-diffusion constant of water at 323 K [82], a known feature of the SPC water model [41]. The values of D_{xy} for the CSLs can be compared with experimental data for solutions of similar concentration and at comparable temperatures (in the absence of lipids). Reasonable agreement is found for MET ($D_{xy} = 2.24 \times 10^{-5}$ compared to $D = 1.37 \times 10^{-5}\,cm^2\,s^{-1}$ at 298.15 K and 0.2 molar fraction, i.e. 13.9 m [83]), ETG ($D_{xy} = 1.52 \times 10^{-5}$ compared to $D = 0.77 \times 10^{-5}\,cm^2\,s^{-1}$ at 298 K and 0.1 molar fraction, i.e. 6.2 m [84]), GLU ($D_{xy} = 0.24 \times 10^{-5}$ compared to $0.14 \times 10^{-5}\,cm^2\,s^{-1}$ at 298 K and 3.7 m [85]) and TRH ($D_{xy} = 0.77 \times 10^{-5}$ compared to $D = 0.151 \times 10^{-5}\,cm^2\,s^{-1}$ at 323 K and 44 wt%, i.e. 2.1 m [82]). The agreement is significantly worse for GLY ($D_{xy} = 1.06 \times 10^{-5}$ compared to $D = 0.26 \times 10^{-5}\,cm^2\,s^{-1}$ at 298 K and

0.0979 molar fraction, i.e. 6.0 m [86]). In the case of TRH, the corresponding numerical value of D_{xy} for water ($2.66 \times 10^{-5}\,cm^2\,s^{-1}$) agrees well with the corresponding experimental result ($D = 1.05 \times 10^{-5}\,cm^2\,s^{-1}$ at 323 K [82]). The higher diffusion of the lipids in the presence of GLU compared to TRH agrees with fluorescence experiments of mixed bilayers in the presence of the two sugars [87]. The above comparisons remain qualitative because the present simulations slightly differ from the quoted experiments in terms of concentration, temperature and presence of the bilayer [82–87]. Keeping this in mind, the simulated systems appear to be too diffusive by a factor 1.4–2.5 for water molecules, and by a factor 1.3–2.0 for the CSL molecules (except GLY and TRH, with factors 4 and 0.5, respectively). The calculated value for the lateral diffusion coefficient of DPPC in the absence of CSL ($D_{xy} = 0.078 \times 10^{-5}\,cm^2\,s^{-1}$) is significantly larger than the corresponding value determined by neutron scattering measurements ($D_{xy} = 0.01 \times 10^{-5}\,cm^2\,s^{-1}$ [88]). This coefficient decreases by about a factor of two, four or seven upon adding MET, GLU or TRH, respectively, and remains approximately the same in the presence of GLY. The particularly high value calculated for ETG is somewhat surprising, and may be a consequence of insufficient statistics (the mean-square positional displacement of DPPC molecules is only approximately linear in time on the 6 ns timescale used for averaging). The diffusivity of water decreases systematically upon increasing the size of the CSL molecule (at constant effective concentration of CSL hydroxyl groups), except for GLU and TRH (nearly identical values). The corresponding value of D_{xy} decrease by a factor of 1.1 (MET), 1.3–1.5 (GLY or ETG) and 1.8 (GLU and TRH) relative to the simulation without CSL. A similar trend is observed for the diffusivity of the different CSLs, which is also systematically reduced upon increasing the size of the CSL molecule. The corresponding value of D_{xy} decreases by a factor of 1.5 (ETG), 2.1 (GLY), 9.3 (GLU) and 29.1 (TRH) relative to the MET solution. Although, the latter dependency shows the expected decrease in solute diffusivity upon increasing the molecular size, the variations are too large to be rationalised on the sole basis of Stoke's law (which also does not account for the trends observed in the water diffusivity). In fact, the above observations probably result from a change in the nature of CSL–CSL and CSL–solvent interactions upon altering the number of hydroxyl groups in the molecule (bulk effect) combined with the specific effect of interactions with the bilayer (interfacial effect; see below).

The distributions of specific DPPC, CSL and water atoms along the bilayer normal, averaged over the final 0.25 ns of the simulations, are shown in Figure 4. The structure of the membrane remains essentially unaffected by the CSLs, except in the presence of MET (Figure 4(b)), where the distributions of the lipid headgroup and GLY atoms are significantly broadened and overlap to a larger extent. This simulation is also the only one characterised by a non-vanishing CSL density in the bilayer interior, suggesting that MET molecules are able to penetrate into this hydrophobic region, in contrast to observations made in a previous simulation [62]. Besides this particularity observed for MET, the profiles evidence a progressive evolution along the series of compounds. On one end of the spectrum, MET (Figure 4(b)) and, to a lesser extent, ETG (Figure 4(c)), show preferential affinity (compared to water) for the superficial region of the bilayer interior (i.e. the local CSL concentration is higher in this region compared to the bulk), but not for the bilayer surface. In other words, these CSLs penetrate more deeply into the bilayer compared to the solvent, but do not present any trend towards clustering at the bilayer surface. This pattern will be further referred to as 'alcohol-like' behaviour. On the other end of the spectrum, TRH (Figure 4(f)) and, to a lesser extent, GLU (Figure 4(e)), show preferential affinity (compared to water) for the bilayer surface, but do not significantly penetrate into the membrane (i.e. not as deeply as the solvent molecules). This preferential affinity is evidenced by the density peaks observed for these CSLs in the vicinity of the bilayer surface, and the overlap between these peaks and those corresponding to DPPC headgroup atoms. Note, however, that water molecules are not completely excluded from the membrane surface upon coating by sugar molecules. The clustering of the sugar molecules may be in part responsible for the limited diffusivity of water and CSL molecules in the TRH and, to a lesser extent, GLU systems (Table 2). This pattern will be further referred to as 'sugar-like' behaviour. In the middle of the series, GLY (Figure 4(d)) presents neither alcohol-like nor sugar-like behaviour, and its local concentration is essentially homogenous throughout the system (i.e. this CSL appears to be inert with respect to the bilayer). Note that the latter observation is at odd with a recent calorimetric study suggesting that GLY is preferentially excluded from the membrane-water interface [41].

Some of the above mentioned features (important lateral expansion of the bilayer, perturbation of its structure and permeation of CSL molecules for MET; membrane coating for GLU and TRH) are clearly visible in the configurations of the systems at the end of the six 15 ns simulations (Figure 5).

The total numbers of H-bonds present on average between the different species in each of the simulated systems (together with the associated fluctuations) are reported in Table 3. Because, the effective concentration of CSL hydroxyl groups is slightly different in the case of GLY and GLU compared to the other systems, an approximate (corrected) estimate for the values corresponding to the exact same effective concentration (17.0 m) is also provided. Quantities derived from this H-bond analysis are also reported in Table 4. Although, the following discussion (as well as Table 4) is based on the

Table 3. Average total numbers of H-bonds between all species within the system, calculated for the six simulations of a DPPC bilayer in the absence or in the presence of different CSLs (Figure 1 and Table 1) at 325 K.

	CSL–DPPC	CSL–CSL	CSL–water	Water–DPPC
No CSL	–	–	–	549 (11)
MET	236 (11)	140 (10)	1354 (28)	356 (17)
ETG	137 (10)	125 (11)	1485 (28)	377 (14)
GLY	77 (9)	144 (12)	1656 (28)	447 (16)
GLY_{corr}	69	128	1472	447
GLU	192 (13)	202 (15)	1644 (30)	350 (15)
GLU_{corr}	154	162	1317	350
TRH	115 (6)	174 (13)	1300 (30)	398 (10)

Note: H-bonds involving the ring (GLU, TRH) and glycosidic (TRH) oxygen atoms are included in the CSL–CSL and CSL–water contributions. The standard deviations are reported between parentheses. The values are averaged over the final 6 ns of the simulations. The corrected values (corr) for the entries involving the CSL in the systems with GLY and GLU are scaled by 0.89 and 0.80 so as to provide an estimate of the corresponding values at an exactly identical effective hydroxyl group concentration compared to the other systems (Table 1).

corrected values for GLY and GLU, the original values present the same qualitative trends.

In the systems involving ETG, GLY, GLU and TRH, the sum of the CSL–DPPC and water–DPPC H-bonds (ALL–DPPC; Table 4) is essentially the same for all CSLs and only slightly lower (ΔALL–DPPC; about 6–8%) than the number of water–DPPC H-bonds in the system without CSL. This suggests that the number of H-bonding (acceptor) sites provided by the membrane is essentially constant (irrespective of the nature of the surrounding solution and of the area per lipid), and that CSLs partially replace water molecules at these H-bonding sites, without significantly altering (i.e. only slightly reducing) the total number of H-bonds between the bilayer surface and its solution environment. In contrast, for the system involving MET, the corresponding sum is slightly higher (by 7.6%) than the number of DPPC–water H-bonds in the system without CSL. This effect will be discussed in more details in the context of the partitioning of H-bonds between lipid phosphate and ester groups (see below). The observation that the total number of H-bonds between the lipids and their environment slightly decreases (6–7%), rather than increases, upon addition of the various CSLs (except with MET) is quite interesting. It suggests that H-bonding to the bilayer is not the driving force underlying the previous observations concerning the area per lipid (Figure 2), order parameters (Figure 3), and density profiles (Figure 4). This interpretation is consistent with the idea that the addition of the CSL does not simply result in the creation of new CSL–lipid H-bonds, *a priori* an energetically very favourable process. Rather, it results in the partial substitution of one type of H-bond donor molecule (water) by another one (CSL) at the bilayer acceptor sites, a process that involves a comparatively much smaller energy change.

As previously observed (Figure 4(b)–(f)), the membrane surface remains extensively hydrated in the presence of all CSLs, even for sugars (which form a dense coating layer). Accordingly, DPPC–water H-bonds still represent the dominant (about 60–85%) contribution to the sum of H-bonds involving DPPC molecules and the surrounding solution (Table 4). The corresponding relative contribution of CSL–DPPC H-bonds (at constant effective concentration of CSL hydroxyl groups) decreases (from about 40 to about 15%) in the order MET $\gg$ GLU $>$ ETG $>$ TRH $\gg$ GLY. The relative variation in the total number of water–DPPC H-bonds upon addition of CSL (Δwater–DPPC; Table 4) indicates that CSL molecules expel about 20–35% of the water molecules from the H-bonding sites provided by the membrane, this fraction decreasing in the sequence GLU $\sim$ MET $>$ ETG $>$ TRH $\gg$ GLY. The presence of H-bonds between CSL molecules and lipid headgroups, as well as the partial replacement of water by

Table 4. Quantities derived from the H-bond analysis for the six simulations of a DPPC bilayer in the absence or in the presence of different CSLs (Figure 1 and Table 1) at 325 K.

	ALL–DPPC	CSL (%)	Water (%)	ΔALL–DPPC (%)	ΔCSL–DPPC (%)	Δwater–DPPC (%)
No CSL	549	0.0	100.0	0.0	–	–
MET	591	39.9	60.1	+7.6	+ 42.9	− 35.3
ETG	514	26.7	73.3	−6.5	+ 25.0	− 31.4
GLY_{corr}	515	13.3	86.7	−6.2	+ 12.5	− 18.7
GLU_{corr}	504	30.5	69.5	−8.2	+ 28.0	− 36.2
TRH	513	22.4	77.6	−6.6	+ 20.9	− 27.5

Note: The quantities reported are the sum of CSL–DPPC and water–DPPC H-bonds (ALL–DPPC), the relative contributions of CSL and water to this total number, the relative variation of this total number with reference to the system in absence of CSL (ΔALL–DPPC), and the relative contributions of CSL (ΔCSL–DPPC) and water (Δwater–DPPC) to this variation. The values are averaged over the final 6 ns of the simulations. The entries for GLY and GLU correspond to corrected values (Table 3).

CSL molecules at the membrane surface, was already reported in experimental studies concerning MET [22], butanol [22] and ethanol [22–24,26], and in several simulation studies concerning MET [60–62], ethanol [59,60,62–64], propanol [64] and butanol [64].

Considering CSL–CSL H-bonds (Table 3), the sugars (GLU, TRH) are seen to have the largest propensity to self H-bonding. This is not surprising considering that sugar molecules tend to aggregate close to the bilayer surface (Figure 4(e),(f) and Figure 5 bottom centre and right). On the other hand, the alcohol and polyols (MET, ETG, GLY), the local concentration of which remains more homogenous throughout the system, show a somewhat lower number of CSL–CSL H-bonds. Expectedly, this trend is inverted when considering the average number of CSL–water H-bonds. The sugars, with a higher tendency for clustering (and more CSL–CSL H-bonds), are also less strongly hydrated (fewer CSL–water H-bonds) compared to the alcohol and polyols.

CSL–DPPC H-bonds involve sugar hydroxyl groups and oxygen acceptors of either the phosphate or the ester group of the lipid molecules. The corresponding contributions are reported in Table 5. In the systems involving ETG, GLY, GLU and TRH, the sums of the CSL–DPPC and water–DPPC H-bonds, divided into contributions associated with the phosphate and ester groups (ALL–DPPC; Table 5), are essentially the same for all CSLs. The phosphate and ester contributions are slightly lower (by about 8–11% and 0–5%, respectively) than the corresponding contributions for water–DPPC H-bonds in the system without CSL. Thus, the slight decrease (about 6–8%; Table 4) observed in the total number of H-bonds involving the bilayer surface and its solution environment corresponds to a slightly more pronounced decrease at the level of the phosphate compared to the ester groups. For MET, the decrease is of similar magnitude as for other CSLs at the level of the phosphate groups (about 10%). However, a large increase is observed at the level of the ester groups (about 22%), resulting in the slight increase (7.6%; Table 4) observed in the total number of H-bonds involving the bilayer surface and its solution environment. MET can thus be singled out in the series of CSLs for its capacity to form H-bonds with (buried) ester sites that are accessible neither to water not to other CSL molecules (thereby, increasing the overall H-bonding capacity of the bilayer).

Besides this peculiarity of MET, the relative contributions of the CSL–ester H-bonds to the total number of CSL–DPPC H-bonds decreases systematically (at constant effective concentration of CSL hydroxyl groups) along the CSL series (from about 60% for MET to only 13% for TRH). This suggests that the contribution of H-bonding to the ester groups is predominantly determined by the molecular size of the CSL, as was the case for the depth of penetration into the bilayer (Figures 4b–f). For the sugars

Table 5. Average total numbers of H-bonds formed between CSL hydroxyl groups or water molecules, as well as their sum (ALL–DPPC), with either the phosphate or the ester groups of the DPPC molecules, calculated for the six simulations of a DPPC bilayer in the absence or in the presence of different CSLs (Figure 1 and Table 1) at 325 K.

	H-bonds to phosphate	H-bonds to ester	H-bonds to phosphate (%)	H-bonds to ester (%)
		CSL–DPPC		
MET	96	140	40.5	59.5
ETG	74	63	53.7	46.6
GLY_{corr}	43	26	62.6	37.4
GLU_{corr}	110	44	71.2	28.8
TRH	99	15	87.0	13.0
		water–DPPC		
No CSL	310	240	56.4	43.6
MET	204	152	57.3	42.7
ETG	211	166	55.9	44.1
GLY	232	215	51.9	48.2
GLU	167	184	47.6	52.4
TRH	184	214	46.2	53.8
		ALL–DPPC		
No CSL	310	240	56.4	43.6
MET	299	292	50.6	49.4
ETG	284	230	55.4	44.7
GLY	275	241	53.3	46.7
GLU	276	228	54.8	45.2
TRH	283	229	55.3	44.8

Note: The relative contributions are also indicated. The values are averaged over the final 6 ns of the simulations. The entries for GLY and GLU in the CSL–DPPC H-bonds correspond to corrected values (Table 3).

(GLU and TRH), the leading contribution is provided by H-bonds to the phosphate groups, in agreement with experimental data on the interaction of sugars with lipid bilayers [79,80,89,90]. However, the presence of a minor component of sugar-ester H-bonds was also reported in previous simulation studies on the interaction of TRH [54,57] and other sugars [57] with phospholipid membranes. The polyols (ETG, GLY) still interact preferentially with the phosphate groups. In contrast, for MET, the proportion of H-bonds to the ester groups becomes dominant. Previous simulation studies have evidenced the formation of H-bonds between the hydroxyl groups of various aliphatic alcohols and both the phosphate [63,64] and the ester groups [64] of the lipids. This observation is also in line with experimental studies [24,26].

The interaction between CSL and DPPC molecules was further characterised by analysing the degree of bridging of the CSL molecules, i.e. the number of distinct DPPC molecules forming at least one H-bond with a given CSL molecule (Table 6). As expected, the occurrences of degrees of bridging higher than the number of hydroxyl groups in a given CSL molecule, which results from the possibility of a single hydroxyl group forming more than one H-bond (given the geometrical H-bonding criterion employed), are very low. For this reason, only sugars can achieve high extents of

Table 6. Average occurrences (in percent) of CSL molecules bridging a specific number of distinct DPPC molecules through (possibly multiple) H-bonds during the simulations of a DPPC bilayer in the absence or in the presence of different CSLs (Figure 1 and Table 1) at 325 K.

	0	1	2	3	4	others
No CSL	–	–	–	–	–	–
MET	77.2	22.7	0.2	–	–	–
ETG	80.1	13.2	6.6	0.1	0.0	–
GLY_{corr}	85.6	9.6	3.9	0.9	0.0	–
GLU_{corr}	62.2	20.5	13.5	3.5	0.3	0.0
TRH	51.6	27.3	14.4	5.8	0.8	0.1

Note: The values are averaged over the final 6 ns of the simulations. A zero indicates molecules forming no H-bonds to DPPC while 'others' indicates CSL molecules H-bonded to five or more distinct DPPC molecules. The entries for GLY and GLU correspond to corrected values (Table 3).

bridging. Configurations where a single TRH or GLU molecule formed as many as six H-bonds with distinct lipid molecules were actually observed in the simulations (Figure 6). The majority of the MET, ETG and GLY molecules (about 77–86%) remain in the bulk, i.e. do not bind to a single lipid molecule. In contrast, a much higher proportion of the GLU and TRH molecules are observed to bind to the lipids (38 and 48%, respectively), which is not only a consequence of the preferential affinity for the membrane surface but also of the higher number of hydroxyl groups per molecule. The occurrences of CSL molecules bound to a single lipid decreases (from about 23 to 7%) in the sequence MET > ETG > GLY. However, the corresponding occurrences of CSL molecules bound to two or more lipids remains low (at most 6.7%). For GLU and TRH, the corresponding occurrences of molecules binding one (20.5 and 27.3%, respectively) and two or more (17.3 and 21.1%, respectively) lipids are significantly higher. Thus, the sugars present a more pronounced tendency to the bridging of multiple lipid molecules (due to the higher number of hydroxyl groups available as H-bonding donors).

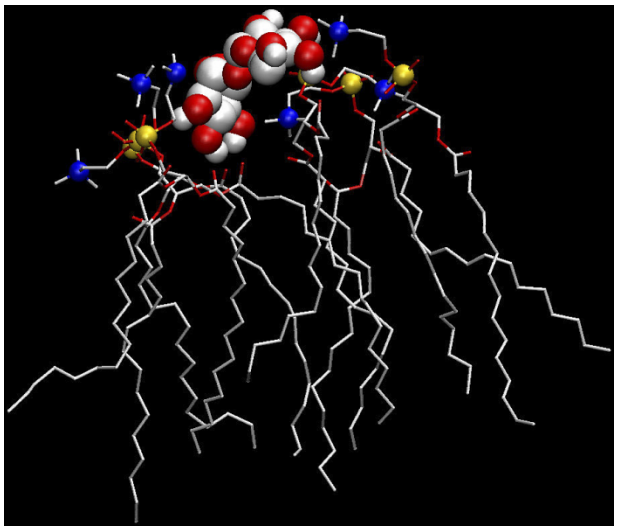

Figure 6. Close up of a configuration sampled during the simulation of a DPPC bilayer in the presence of TRH (Figure 1 and Table 1) at 325 K, illustrating a TRH molecule simultaneously H-bonded to six distinct lipid molecules. TRH is represented using a spacefill model and the DPPC molecules using a stick model. Nitrogen and phosphorous atoms are represented using a spacefill model to better distinguish the lipid headgroups.

4. Discussion

The trends observed along the series of polyhydroxylated compounds considered (at constant hydroxyl group concentration) were found to be systematic neither in terms of increasing molecular size nor among different observables. This suggests that the phenomena taking place in these systems are considerably more complex than initially anticipated, and may involve several mechanisms rather than a common one.

The analyses of the density profiles for the different simulations (Figure 4), which exhibit systematic trends along the CSL series, led us to introduce the concepts of alcohol-like and sugar-like behaviours. Alcohol-like behaviour, shown by MET and, to a lesser extent, ETG, is defined as a preferential affinity of the CSL (compared to water) for the superficial region of the bilayer interior. Sugar-like behaviour, shown by TRH and, to a lesser extent, GLU, is defined as a preferential affinity of the CSL (compared to water) for the bilayer surface. Based one these definitions, GLY presents neither the former nor the latter type of behaviour (i.e. it is inert with respect to the membrane). The other analyses performed for the different simulations show less systematic trends along the CSL series, with the exception of the fraction of CSL–DPPC H-bonds contributed by the ester groups (Table 5), and the extent of lipid bridging by H-bonded CSL molecules (Table 6).

Alcohol-like behaviour appears to correlate with the following effects (typically more pronounced for MET compared to ETG): (1) a significant lateral expansion of the bilayer (Figure 2); (2) a decrease in the order parameters for the lipid acyl chains (Figure 3); (3) a deeper penetration of the CSL molecules (compared to water) into the bilayer interior, but no preferential affinity for the membrane surface (Figure 4); (4) a more extensive substitution of water molecules at the H-bonding sites provided by the membrane (Table 4; about 32–35% water–DPPC H-bond replaced by about 25–43% CSL–DPPC H-bonds); (5) a more extensive substitution of water molecules at the level of the ester as opposed to the phosphate groups (Table 5); (6) a more limited extent of H-bonded bridging of the lipid molecules (Table 6).

Sugar-like behaviour appears to correlate with the following effects (typically more pronounced for TRH compared to GLU): (1) no significant lateral expansion of the bilayer (TRH only; Figure 2); (2) no significant change in the

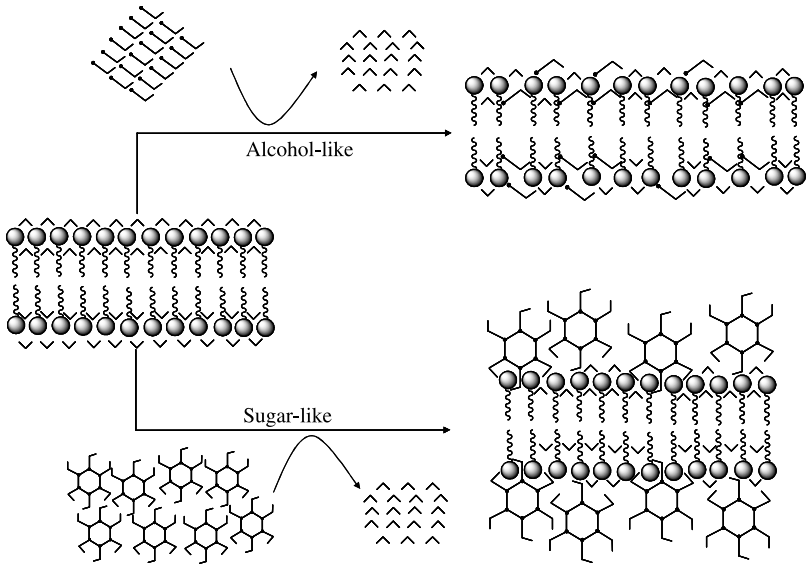

Figure 7. Schematic representation illustrating the key features of the alcohol-like and sugar-like mechanisms. Lipids are symbolised by a sphere (headgroup) and a tail (glycerol plus two acyl chains), alcohol molecules by MET, and sugar molecules by a polyhydroxylated six-membered ring. CSL aliphatic groups are drawn as small black spheres, and the corresponding hydroxyl groups using lines. Water molecules are drawn using lines. In the alcohol-like mechanism, the CSL shows preferential affinity for the superficial region of the bilayer interior and partially substitutes water molecules by H-bonding to the lipids, predominantly at the level of the ester groups. The driving force is the hydrophobic effect (transfer of CSL molecules from the bulk to a less polar environment and simultaneous transfer of water molecules from this less polar environment to the bulk). In the sugar-like mechanism, the CSL shows preferential affinity for the bilayer surface (where it tends to aggregate) and partially substitutes water molecules by H-bonding to the lipids, predominantly at the level of the phosphate groups. The driving force is entropic (release of many water molecules to the bulk at the cost of immobilising and rigidifying fewer CSL molecules, already inherently rigid).

order parameters for the lipid acyl chains (TRH only; Figure 3); (3) a more limited penetration of the CSL molecules (compared to water) into the bilayer and the formation of a dense coating layer (still significantly hydrated) of CSL molecules at the membrane surface (Figure 4); (4) a more limited replacement of water molecules at the H-bonding sites provided by the membrane (TRH only, Table 5); (5) a more extensive replacement of water molecules at the level of the phosphate as opposed to the ester groups (Table 5); (6) a more extensive H-bonded bridging of the lipid molecules (Table 6).

The above correlations are very clear for MET, ETG and TRH. MET also presents some unique properties compared to all the other solutes investigated: a permeation through the membrane, a significant perturbation of the bilayer structure (Figures 4(b) and 5 top centre) and the capacity to form H-bonds with (buried) ester sites that are accessible neither to water nor to the other CSL molecules (Table 5). The case of GLU appears to be somewhat intermediate in that it deviates from the expectations for sugar-like behaviour (being more alcohol-like) with respect to properties (1), (2) and (4). Finally, although, GLY does formally fit neither the definition of alcohol-like nor of sugar-like behaviour (limited penetration into the bilayer but no preferential affinity for its surface), it presents most of the characteristics of sugar-like behaviour, except for properties (3) and (6).

One of the principal difficulties when investigating (both experimentally and theoretically) complex molecular systems of the kind considered here is to interpret observed correlations between the observables monitored (see above) in terms of causality sequences. However, we believe that the present results (along with the available experimental data) provide hints (if not a definitive proof) supporting the following interpretation, relying on the existence of two distinct mechanisms for the interaction of polyhydroxylated compounds with membranes. These will be furthered referred to as alcohol-like and sugar-like mechanisms (Figure 7), respectively.

Aliphatic alcohols are significantly less polar than water (for example, the relative dielectric permittivity of liquid MET is 33.0 compared to 80.1 for water [91]). However, under bulk conditions, short-chain alcohols (up to propanol) remain miscible with water in all proportions at room temperature because the hydrophobic effect (which should promote phase separation) does not compensate for the dessolvation penalty of the hydroxyl groups (amphiphilic balance) and the entropy of mixing. The situation is different in the vicinity of a lipid bilayer (i.e. for an interfacial system). Alcohol molecules that are either small (e.g. MET, ethanol, ETG) or flexible (e.g.

longer-chain aliphatic alcohols) enough to reach the lower polarity environment of the lipid glycerol groups (or even of the lipid tails), while preserving polar interactions with the phosphate and ester groups (as well as with water), will tend to cluster in this region, where their chemical potential relative to the bulk is lower than that of water. As a consequence, they partially substitute water molecules at the H-bonding sites provided by the membrane (the total number of which appears to be essentially constant, irrespective of nature and concentration of the CSL and the degree of expansion of the bilayer; MET representing an exception), and predominantly those associated with the ester groups. Because alcohols are bulkier than water and can only donate a single H-bond per hydroxyl group (as opposed to two H-bonds for a water molecule), the effective volume of the alcohol–water mixture required to achieve saturation of the membrane H-bonding sites is larger than the corresponding effective water volume in the absence of CSL. Consequently, the membrane undergoes lateral expansion (and a concomitant decrease in the order of the lipid tails). A key point of this suggested mechanism is that H-bonding is not the driving force underlying the preferential affinity of alcohol molecules for the superficial region of the bilayer interior. Rather, it is the favourable change in free energy associated with the substitution of a H-bonding water molecule by a H-bonding alcohol molecule in this (less polar) environment, including the contributions associated with the transfer of the two molecules to and from the (more polar) bulk solution. Here, H-bonding to the lipids merely plays the role of a constraint on the total number of (CSL plus water) H-bonding groups, which must remain approximately constant to avoid the enthalpic penalty associated with unsatisfied lipid H-bonding sites. According to this mechanism, alcohol, polyol or sugar molecules that are too bulky or too rigid to reach deep into the bilayer should essentially be inert to the membrane (its outer surface being of similar polarity as the bulk solution). This mechanism is compatible with the experimentally observed proportionality between the lateral expansion of the membrane and the alcohol concentration [28]. For aliphatic alcohols, this alcohol-like behaviour is likely to be modulated by the length of the aliphatic tail. A longer tail is expected to enhance the hydrophobicity of the molecule leading to an affinity enhancement with, in the limit of long chains, the possible insertion of the tail into the membrane hydrophobic core [32]. For polyols, the mechanism may be complicated by the requirement of finding multiple simultaneous H-bonding partners for a single CSL molecule. Finally, the present alcohol-like mechanism is supported by experimental evidence concerning the location of ethanol molecules in phospholipid membranes [23,26] and by the results of independent simulation studies on the influence of alcohols on membranes [59,64].

Although, the alcohol-like mechanism alone seems to imply that large polyhydroxylated CSLs (e.g. sugars) should be inert with respect to lipid bilayers, a distinct effect may come into play in this case. Due to their size, sugar molecules cannot penetrate deep into the membrane. Still, they can also partially substitute water molecules at the H-bonding sites provided by the membrane (the number of which appears to be essentially constant also here), and predominantly at those associated with the phosphate groups. The substitution of water may be somewhat unfavourable enthalpically (because the positions and orientations of the sugar hydroxyl groups are constrained by the molecular framework and stereochemistry, leading to suboptimal H-bonding geometries). However, it is expected to be extremely favourable entropically because each sugar molecule is capable of replacing multiple (highly ordered) water molecules at the bilayer surface, releasing them into the bulk solution. This substitution may also involve an entropic cost associated with restraints imposed on the sugar intramolecular degrees of freedom upon binding (e.g. freezing of glycosidic linkages). However, this cost is likely to be small because sugars are inherently rather rigid molecules. According to this mechanism, membrane coating by sugars (unlike membrane penetration by alcohols) should have little effect on the area per lipid and order parameters. Here also, a key point of the suggested mechanism is that H-bonding is not the driving force underlying the preferential affinity of sugar molecules for the membrane surface. Rather, it is the large entropy gain associated with the release of many molecular translational and rotational degrees of freedom (water molecules), which is only slightly reduced by the limited entropy cost of immobilising and rigidifying fewer sugar molecules. Again, H-bonding to the lipid molecules merely represents a constraint (of enthalpic origin) on the total number of (CSL plus water) H-bonding groups interacting with the membrane, which must remain approximately constant during the substitution process. Note that this substitution does not need to involve all hydroxyl groups of a sugar molecule. Intermediate situations are actually more likely, where sugar molecules substitute water molecules at the H-bonding sites for which their hydroxyl groups are well positioned, while water molecules provide the remaining H-bonds for saturating the bilayer sites. Note also that the present sugar-like mechanism has been formulated in the context of moderately dilute solutions. In the concentrated regime (or upon dehydration) the situation may be altered by the formation of a glassy state (vitrification of the sugar matrix).

Among the different polyhydroxylated CSLs considered, MET and ETG clearly fit the expected properties for an alcohol-like mechanism (most pronounced for the smaller molecule), while TRH fits those expected for a sugar-like mechanism. The cases of GLY and GLU are somewhat less clear and present characteristics of both

situations. GLY shows neither alcohol-like nor sugar-like behaviour and is essentially inert with respect to the membrane. In addition, as mentioned above, the alcohol-like mechanism may not be strictly applicable to polyols (at least beyond ETG). The case of GLU is somewhat puzzling. This CSL shows most properties of a sugar-like behaviour. However, it still promotes a lateral expansion of the bilayer and a disorder increase in the lipid tails, although these features cannot be related to the alcohol-like mechanism (no significant penetration into the bilayer, limited interaction with the ester groups). We have at the moment no satisfactory explanation for the behaviour of this CSL.

The proposed sugar-like mechanism has a number of interesting consequences concerning the interaction of oligosaccharides with membranes (under normal conditions of temperature and hydration). First, it suggests that the preferential affinity for the bilayer surface may be affected by a complex interplay between two main factors: the size of the sugar molecule and its intrinsic flexibility. Increasing the size of the molecule increases the number of hydroxyl groups per molecule and thus, in principle, the magnitude of the entropy gain upon sugar binding (suggesting an affinity enhancement). However, it probably also decreases the density of surface coating (larger oligosaccharides are likely to pack less efficiently) and increases the geometrical constraints imposed on the hydroxyl group positions and orientations by the molecular framework, which may in effect limit the extent of water replacement at the membrane surface (suggesting an affinity decrease). Increasing the flexibility of the molecule (e.g. by changing the nature of the residues or glycosidic linkages) increases the entropy cost of partially freezing its internal degrees of freedom upon binding (suggesting an affinity decrease), but also probably increases the density of surface coating, extent of water substitution and optimality of sugar–lipid H-bonding geometries (suggesting an affinity increase). Finally, in the context of oligosaccharides, molecular size and flexibility are intimately correlated, since most of the flexibility of these compounds resides in the glycosidic linkages [92–94].

Second, the sugar-like mechanism suggests an explanation for the sugar-mediated bioprotection of membranes under dehydrating conditions [5–7]. The entropically-driven (partial) replacement of water–lipid H-bonds by sugar–lipid H-bonds leads to a H-bonded cross-linking of the individual lipids. Under normal conditions, this cross-linking is likely to have a limited influence on the bilayer properties, because the involved H-bonds will be quite labile in an aqueous environment. However, the dehydration of the system is expected to lead to a dramatic enhancement in the stability of sugar–lipid H-bonded interactions (by removal of the competing water molecules or, equivalently, reduction of dielectric screening effects). This scaffold of sugar molecules bridging the lipids (together with the vitrification of the sugar matrix) may provide an enhanced resistance against mechanical disruption and prevent a transition to the gel phase by preserving the spacing between the lipid headgroups. This would also explain why sugars have no remarkable effect on bilayers in the dilute regime but become 'active' (in terms of bioprotection) upon dehydration [6]. Note that the preferential interaction of sugars with membrane surfaces and their binding to the headgroups have been suggested previously as a possible reason for the stabilisation of membranes under dehydration conditions [5,6,13,17,39]. Somewhat surprisingly, however, sugars have been suggested to be preferentially excluded from the surface of proteins, both by experiments in the dilute [95] or concentrated regime [14,96] and by simulations in moderately concentrated solutions [97,98]. But it should be stressed that this issue remains matter of debate [99].

5. Conclusions

The aim of the present study was to investigate and compare the interaction of different polyhydroxylated CSLs with a hydrated DPPC bilayer using MD simulations at 325 K. It should be kept in mind that the reported observations are in principle only relevant for systems compared at a constant effective concentration of hydroxyl groups and to the concentration regime considered. Furthermore, one should realise that the present systems are ternary systems (lipid–CSL–water, i.e. involving two independent concentration variables at constant pressure and temperature), at a very high effective concentration of lipids. This means in practice that surface effects (e.g. penetration of the membrane by alcohol molecules or coating of the membrane by sugar molecules) significantly affect the concentration of the surrounding solution. For example, if the preferential affinity of the CSL for some region of the bilayer is very high, it may (almost) entirely deplete the surrounding bulk solution from CSL molecules, in which case the simulation describes a CSL-associated bilayer in equilibrium with (almost) pure water, rather than in equilibrium with a solution at the specified concentration. Finally, it should be noted that the force field employed leads to a somewhat underestimated value of the area per lipid of a fully hydrated DPPC bilayer ($0.57\,nm^2$) compared to experiment ($0.64\,nm^2$ [78]). This may somewhat affect the quantitative results of the present study (possibly by reducing the penetration of CSLs into the bilayer). However, it is unlikely to significantly affect the qualitative conclusion of the present work (in terms of trends along the CSL series).

Keeping these restrictions in mind, the present simulation results (together with available experimental data) led to the formulation of two mechanisms for the interaction of polyhydroxylated compounds with lipid bilayers. The alcohol-like mechanism, active for MET and ETG (and, presumably, other aliphatic alcohols), involves preferential affinity of the CSL molecules for the

superficial region of the bilayer interior, mainly driven by the hydrophobic effect. It results in the lateral expansion of the bilayer, an increase in the disorder of the lipid acyl chains and the partial substitution of water–lipid by CSL–lipid H-bonds, predominantly at the level of the ester groups. The sugar-like mechanism, active for GLU and TRH (and, presumably, other mono- and oligosaccharides), involves a preferential affinity of the CSL molecules for the membrane surface (i.e. CSL clustering and coating of the bilayer), mainly driven by entropic effects. It does not result in significant changes in the area per lipid and order parameters of the lipid acyl chains and involves the substitution of water–lipid by CSL–lipid H-bonds, predominantly at the level of the phosphate groups. Furthermore, it results in the H-bonded bridging of the lipids by the CSL molecules, which may have implications in the context of membrane bioprotection by sugars.

A common key feature of both suggested mechanisms is that CSL–lipid H-bonding is not the driving force for the observed effects. This suggestion is supported by the simulation results with the observation that in all but one case (MET), the total number of H-bonds between the lipid bilayer and its solution environment (solvent and CSL) slightly decreases compared to the pure water environment. Such a decrease can only be understood if it is compensated by favourable effects of another nature (hydrophobic or entropic in the present case).

A second key feature is the near constancy of the number of H-bonds formed between the membrane and its environment (irrespective of the nature of the CSL and the area per lipid). This observation is probably related to two specific properties of these systems: (i) phosphate and esters groups can only function as H-bond acceptors, i.e. they cannot form H-bonds with each other and only rely on the surrounding solution for finding appropriate H-bonding partners; (ii) these groups are already almost fully saturated in H-bonds in pure water, so that a possible lateral expansion in the presence of a CSL or a deep penetration of the CSL molecules into the membrane does not expose additional sites. Note, however, that MET represents an exception to the last statement.

Although, the two above suggested mechanisms are compatible with many observations from experiments and simulations (including the present ones), they still only represent hypotheses. Further work will be needed to asses the validity of these principles, possibly first in the context of simpler model systems.

Acknowledgements

Financial support by the Swiss National Foundation, grant #21-105397, is gratefully acknowledged. The authors would like to thank Daan Geerke for making the parameters for ETG and GLY available to them.

References

[1] G.M. Cooper, R.E. Hausman, *The Cell: a Molecular Approach*, ASM Press, Washington, DC, 2007.
[2] L. Yeagle, ed., *The Structure of Biological Membranes*, CRC Press, Boca Raton, FL, 2005.
[3] G.R.A. Hunt and I.C.A. Jones, *^{1H}NMR investigation of the effects of ethanol and general anesthetics on ion channels and membrane fusion using unilamellar phospholipids membranes*, Biochim. Biophys. Acta. 736 (1983), p. 1.
[4] W.R. Klemm, *Biological water and its role in the effect of alcohol*, Alcohol 15 (1998), p. 249.
[5] L.M. Crowe, *Lessons from nature: the role of sugars in anhydrobiosis*, Comp. Biochem. Physiol. A. 131 (2002), p. 505.
[6] J.H. Crowe et al., *Stabilization of dry mammalian cells: lessons from nature*, Integr. Comp. Biol. 45 (2005), p. 810.
[7] A. Tunnacliffe and J. Lapinski, *Resurrecting van Leeuwenhoek's rotifers: a reappraisal of the role of disaccharides in anhydrobiosis*, Philos. Trans. R. Soc. B. 358 (2003), p. 1755.
[8] N. Franks and W.R. Lieb, *Partitioning of long-chain alcohols into lipid bilayers: implications for mechanisms of general anesthesia*, PNAS 83 (1986), p. 5116.
[9] J.T. Mohr et al., *Anesthetic potency of two novel synthetic polyhydric alkanols longer than the* n*-alkanol cutoff: evidence for a bilayer-mediated mechanism of anesthesia?* J. Med. Chem. 48 (2005), p. 4172.
[10] R.S. Cantor, *The lateral pressure profile in membranes: a physical mechanism of general anesthesia*, Biochemistry 36 (1997), p. 2339.
[11] B.J. Fuller, *Cryoprotectants: the essential antifreezes to protect life in the frozen state*, Cryoletters 25 (2004), p. 375.
[12] Z. Hubalek, *Protectants used in the cryopreservation of microorganisms*, Cryobiology 46 (2003), p. 205.
[13] J.H. Crowe, J.S. Clegg, and L.M. Crowe, *Anhydrobiosis: the water replacement hypothesis*, in *The Properties of Water in Foods*, (ISOPOW 6) D.S. Reid ed., Chapman and Hall, New York, 1998, pp. 440–455.
[14] S. Belton and A.M. Gil, *IR and Raman-spectroscopic studies of the interaction of trehalose with hen egg-white lysozyme*, Biopolymers 34 (1994), p. 957.
[15] W.Q. Sun and A.C. Leopold, *Cytoplasmic vitrification acid survival of anhydrobiotic organisms*, Comp. Biochem. Physiol. A. 117 (1997), p. 327.
[16] J.S. Clegg, *Cryptobiosis – a peculiar state of biological organization*, Comp. Biochem. Physiol. B. 128 (2001), p. 613.
[17] J.H. Crowe, J.F. Carpenter, and L.M. Crowe, *The role of vitrification in anhydrobiosis*, Annu. Rev. Physiol. 60 (1998), p. 73.
[18] I. Ueda and T. Yoshida, *Hydration of lipid membranes and the action mechanisms of anesthetics and alcohols*, Chem. Phys. Lipids 101 (1999), p. 65.
[19] N.P. Franks, *Molecular targets underlying general anaesthesia*, Br. J. Pharmacol. 147 (2006), p. S72.
[20] E.S. Rowe, *Lipid chain-length and temperature-dependence of ethanol phosphatidylcholine interactions*, Biochemistry 22 (1983), p. 3299.
[21] S.A. Simon and T.J. McIntosh, *Interdigitated hydrocarbon chain packing causes the biphasic transition behavior in lipid alcohol suspensions*, Biochim. Biophys. Acta. 773 (1984), p. 169.
[22] J.-S. Chiou et al., *Alcohols dehydrate lipid membranes: an infrared study on hydrogen bonding*, Biochim. Biophys. Acta. 1110 (1992), p. 225.
[23] J.A. Barry and K. Gawrisch, *Direct NMR evidence for ethanol binding to the lipid–water interface of phospholipid bilayers*, Biochemistry 33 (1994), p. 8082.
[24] S.E. Feller et al., *Nuclear overhauser enhancement spectroscopy cross-relaxation rates and ethanol distribution across membranes*, Biophys. J. 82 (2002), p. 1396.
[25] L. Löbbecke and G. Cevc, *Effects of short-chain alcohols on the phase behavior and interdigitation of phosphatidylcholine bilayer membranes*, Biochim. Biophys. Acta. 1237 (1995), p. 59.
[26] L.L. Holte and K. Gawrisch, *Determining ethanol distribution in phospholipid multilayers with MAS-NOESY spectra*, Biochemistry 36 (1997), p. 4669.

[27] H.V. Ly, D.E. Block, and M.L. Longo, *Interfacial tension effect of ethanol and lipid bilayer rigidity, stability, and area/molecules: a micropipette aspiration approach*, Langmuir 18 (2002), p. 8988.

[28] H.V. Ly and M.L. Longo, *The influence of short-chain alcohols on the interfacial tension, mechanical properties, area/molecules, and permeability of fluid lipid bilayers*, Biophys. J. 87 (2004), p. 1013.

[29] T.J. McIntosh et al., *The effect of ethanol on the phase transition temperature and the phase structure of monounsaturated phosphatidylcholines*, Biochim. Biophys. Acta. 1510 (2001), p. 219.

[30] K. Ohki, K. Tamura, and I. Hatta, *Ethanol induces interdigitated gel phase ($l_{\beta i}$) between lamellar gel phase ($l_{\beta'}$) and ripple phase ($p_{\beta'}$) in phosphatidylcholine membranes: a scanning density meter study*, Biochim. Biophys. Acta. 1028 (1990), p. 215.

[31] J. Mou et al., *Alcohol induces interdigitated domains in unilamellar phosphatidylcholine bilayers*, Biochemistry 33 (1994), p. 9981.

[32] W. Westerman et al., *The interaction of* n*-alkanols with lipid bilayer membranes: a 2H-NMR study*, Biochim. Biophys. Acta. 939 (1988), p. 64.

[33] R.V. McDaniel, T.J. McIntosh, and S.A. Simon, *Nonelectrolyte substitution for water in phosphatidylcholine bilayers*, Biochim. Biophys. Acta. 731 (1983), p. 97.

[34] M.J. Swamy and D. Marsh, *Thermodynamics of interdigitated phases of phosphatidylcholine in glycerol*, Biophys. J. 69 (1995), p. 1402.

[35] W. Williams et al., *The effects of glycerol on the phase-behavior of hydrated distearoylphosphatidylethanolamine and its possible relation to the mode of action of cryoprotectants*, Biochim. Biophys. Acta. 1062 (1991), p. 123.

[36] M. Yamazaki et al., *Phase-transitions of phospholipid-vesicles under osmotic-stress and in the presence of ethylene–glycol*, Biophys. Chem. 43 (1992), p. 29.

[37] K. Nicolay, E.B. Smaal, and B. Dekruijff, *Ethylene–glycol causes acyl chain disordering in liquid–crystalline, unsaturated phospholipid model membranes, as measured by h-2 NMR*, FEBS Lett. 209 (1986), p. 33.

[38] B. Bechinger, M. Macdonald, and J. Seelig, *Deuterium NMR-studies of the interactions of polyhydroxyl compounds and of glycolipids with lipid model membranes*, Biochim. Biophys. Acta. 943 (1988), p. 381.

[39] J.H. Crowe et al., *Are freezing and dehydration similar stress vectors – a comparison of modes of interaction of stabilizing solutes with biomolecules*, Cryobiology 27 (1990), p. 219.

[40] T.J. Anchordoguy et al., *Modes of interaction of cryoprotectant with membrane phospholipids during freezing*, Biophys. J. 51 (1987), p. A163.

[41] P. Westh, *Unilamellar DMPC vesicles in aqueous glycerol: preferential interactions and thermochemistry*, Biophys. J. 84 (2003), p. 341.

[42] A.H. de Vries, A.E. Mark, and S.J. Marrink, *Molecular dynamics simulation of the spontaneous formation of a small DPPC vesicle in atomistic detail*, J. Am. Chem. Soc. 126 (2004), p. 4488.

[43] A.H. de Vries et al., *Molecular structure of the lecithin ripple phase*, PNAS 102 (2005), p. 5392.

[44] R. Baron et al., *Configurational entropies of lipids in pure and mixed bilayers from atomic-level and coarse-grained simulations*, J. Phys. Chem. B. 110 (2006), p. 15602.

[45] L.R. Forrest and M.S. Sansom, *Membrane simulations: Bigger and better?* Curr. Opin. Struct. Biol. 10 (2000), p. 174.

[46] M.L. Berkowitz, D.L. Bostick, and S. Pandit, *Aqueous solutions next to phospholipid membrane surfaces: insights from simulations*, Chem. Rev. 106 (2006), p. 1527.

[47] A.K. Sum and J.J. de Pablo, *Molecular simulation study on the influence of dimethylsulfoxide on the structure of phospholipid bilayers*, Biophys. J. 85 (2003), p. 3636.

[48] K.C. Tu et al., *Effects of anesthetics on the structure of a phospholipid bilayer: molecular dynamics investigation of halothane in the hydrated liquid crystal phase of dipalmitoylphosphatidylcholine*, Biophys. J. 75 (1998), p. 2123.

[49] ———, *Distribution of halothane in a dipalmitoylphosphatidylcholine bilayer from molecular dynamics calculations*, Biophys. J. 78 (2000), p. 800.

[50] P. Tang and Y. Xu, *Large-scale molecular dynamics simulations of general anesthetic effects on the ion channel in the fully hydrated membrane: the implication of molecular mechanisms of general anesthesia*, PNAS 99 (2002), p. 16035.

[51] Z.W. Liu, Y. Xu, and P. Tang, *Molecular dynamics simulations of C_2F_6 effects on gramicidin a: implications of the mechanisms of general anesthesia*, Biophys. J. 88 (2005), p. 3784.

[52] A.K. Sum, R. Faller, and J.J. de Pablo, *Molecular simulation study of phospholipid bilayers and insights of the interactions with disaccharides*, Biophys. J. 85 (2003), p. 2830.

[53] C.S. Pereira et al., *Interaction of the disaccharide trehalose with a phospholipid bilayer: a molecular dynamics study*, Biophys. J. 86 (2004), p. 2273.

[54] M.A. Villarreal et al., *Molecular dynamics simulation study of the interaction of trehalose with lipid membranes*, Langmuir 20 (2004), p. 7844.

[55] A. Skibinsky, R.M. Venable, and R.W. Pastor, *A molecular dynamics study of the response of lipid bilayers and monolayers to trehalose*, Biophys. J. 89 (2005), p. 4111.

[56] S. Leekumjorn and A.K. Sum, *Molecular investigation of the interactions of trehalose with lipid bilayers of DPPC, DPPE and their mixture*, Mol. Simul. 32 (2006), p. 219.

[57] C.S. Pereira and P.H. Hünenberger, *Interaction of the sugars trehalose, maltose and glucose with a phospholipid bilayer: a comparative molecular dynamics study*, J. Phys. Chem. B. 110 (2006), p. 15572.

[58] ———, *The effect of trehalose on a phospholipid membrane under mechanical stress*, submitted to Biophys. J.

[59] J. Chanda and S. Bandyopadhyay, *Distribution of ethanol in a model membrane: a computer simulation study*, Chem. Phys. Lett. 392 (2004), p. 249.

[60] B.W. Lee et al., *Structural effects of small molecules on phospholipid bilayers investigated by molecular simulations*, Fluid Phase Equilib. 225 (2004), p. 63.

[61] D. Pinisetty, D. Moldovan, and R. Devireddy, *The effect of methanol on lipid bilayers: an atomistic investigation*, Ann. Biomed. Eng. 34 (2006), p. 1442.

[62] M. Patra et al., *Under the influence of alcohol: the effect of ethanol and methanol on lipid bilayers*, Biophys. J. 90 (2006), p. 1121.

[63] J. Chanda and S. Bandyopadhyay, *Perturbation of phospholipid bilayer properties by ethanol at a high concentration*, Langmuir 22 (2006), p. 3775.

[64] A.N. Dickey and R. Faller, *How alcohol chain-length and concentration modulate hydrogen bond formation in a lipid bilayer*, Biophys. J. 92 (2007), p. 2366.

[65] W.F. van Gunsteren et al. *Biomolecular Simulation: the GROMOS96 manual and user guide. Hochschulverlag an der ETH Zürich/Biomos, Zürich/Groningen*, (1996)

[66] R.D. Lins and P.H. Hünenberger, *A new GROMOS force field for hexopyranose-based carbohydrates*, J. Comput. Chem. 26 (2005), p. 1400.

[67] I. Chandrasekhar et al., *A consistent potential energy parameter set for lipids: dipalmitoylphosphatidylcholine as a benchmark of the GROMOS96 45A3 force field*, Eur. Biophys. J. 32 (2003), p. 67.

[68] C.S. Pereira et al., *Conformational and dynamical properties of disaccharides in water: a molecular dynamics study*, Biophys. J. 90 (2006), p. 4337.

[69] V. Kräutler, M. Müller, and H. Hünenberger, *Conformation, dynamics, solvation and relative stabilities of selected beta-hexopyranoses in water: a molecular dynamics study with the GROMOS 45A4 force field*, Carbohydr. Res., 42 (2007), 2097.

[70] H.J.C. Berendsen et al., *Interaction models for water in relation to protein hydration*, in *Intermolecular Forces*, B. Pullman ed., Reidel, Dordrecht, 1981, pp. 331–342.

[71] D.P. Geerke and W.F. van Gunsteren, *The performance of non-polarizable and polarizable force-field parameter sets for ethylene glycol in molecular dynamics simulations of the pure liquid and its aqueous mixtures*, Mol. Phys. 1005 (2007), p. 1861.

[72] R.W. Hockney, *The potential calculation and some applications*, Methods Comput. Phys. 9 (1970), p. 136.

[73] J. Ryckaert, G. Ciccotti, and H.J.C. Berendsen, *Numerical integration of cartesian equations of motion of a system with constraints molecular dynamics of* n*-alkanes*, J. Comput. Phys. 23 (1977), p. 327.

[74] H.J.C. Berendsen et al., *Molecular dynamics with coupling to an external bath*, J. Chem. Phys. 81 (1984), p. 3684.
[75] W.F. van Gunsteren and H.J.C. Berendsen, *Computer simulation of molecular dynamics: methodology, applications and perspectives in chemistry*, Angew. Chem. Int. Ed. Engl. 29 (1990), p. 992.
[76] I.G. Tironi et al., *A generalized reaction field method for molecular dynamics simulations*, J. Chem. Phys. 102 (1995), p. 5451.
[77] A.H. de Vries et al., *Molecular dynamics simulations of phospholipid bilayers: influence of artificial periodicity, system size, and simulation time*, J. Phys. Chem. B 109 (2005), p. 11643.
[78] J.F. Nagle and S. Tristam-Nagle, *Structure of lipid bilayers*, Biochim. Biophys. Acta. 1469 (2000), p. 159.
[79] M.D. Luzardo et al., *Effect of trehalose and sucrose on the hydration and dipole potential of lipid bilayers*, Biophys. J. 78 (2000), p. 2452.
[80] H. Takahashi, H. Ohmae, and I. Hatta, *Trehalose-induced destabilization of interdigitated gel phase in dihexadecylphosphatidylcholine*, Biophys. J. 73 (1997), p. 3030.
[81] J. Douliez, A. Leonard, and E.J. Dufourc, *Restatement of order parameters in biomembranes – calculation of C—C bond order parameters from C–D quadrupolar splittings*, Biophys. J. 68 (1995), p. 1727.
[82] N. Ekdawi-Sever et al., *Diffusion of sucrose and alpha,alpha-trehalose in aqueous solutions*, J. Phys. Chem. A 107 (2003), p. 936.
[83] Z.J. Derlacki et al., *Diffusion-coefficients of methanol and water and the mutual diffusion-coefficient in methanol water solutions at 278 K and 298 K*, J. Phys. Chem. 89 (1985), p. 5318.
[84] L. Ambrosone et al., *Dynamic properties of aqueous solutions of ethylene glycol oligomers as measured by the pulsed gradient spin-echo NMR technique at 25°C*, J. Chem. Soc. Faraday Trans. 93 (1997), p. 3961.
[85] M. Castaldi, G. D'Errico, L. Paduano, and V. Vitagliano, *Transport properties of the binary system glucose–water at 25 degrees C. A velocity correlation study*, J. Chem. Eng. Data 43 (1998), p. 653.
[86] G. D'Errico, O. Ortona, F. Capuano, and V. Vitagliano, *Diffusion coefficients for the binary system glycerol plus water at 25 degrees C. A velocity correlation study*, J. Chem. Eng. Data 49 (2004), p. 1665.
[87] G. van den Bogaart et al., *On the decrease in lateral mobility of phospholipids by sugars*, Biophys. J. 92 (2007), pp. 1598–1605.
[88] E. Sackmann, in *Handbook of Biological Physics, Structure and Dynamics of Membranes*, R. Lipowsky & E. Sackman, eds.,Vol. 1A, Elsevier, Amsterdam, 1995, pp. 213–304.
[89] D.K. Hincha and M. Hagemann, *Stabilization of model membranes during drying by compatible solutes involved in the stress tolerance of plants and microorganisms*, Biochem. J. 383 (2004), p. 277.
[90] J.H. Crowe et al., *Stabilization of dry membranes by mixtures of hydroxyethyl starch and glucose: the role of vitrification*, Cryobiology 35 (1997), p. 20.
[91] D.R. Lide, ed., in *CRC Handbook of Chemistry and Physics*, CRC Press, Boca Raton, FL, 2001.
[92] C. Cacela and D.K. Hincha, *Monosaccharide composition, chain length and linkage type influence the interactions of oligosaccharides with dry phosphatidylcholine membranes*, Biochim. Biophys. Acta Biomem. 1758 (2006), p. 680.
[93] I.J. Vereyken et al., *The effect of fructan on the phospholipid organization in the dry state*, Biophys. J. 85 (2003), p. 3058.
[94] ——— et al., *Structural requirements of the fructan–lipid interaction*, Biophys. J. 84 (2003), p. 3147.
[95] S.N. Timasheff, *Control of protein stability and reactions by weakly interacting cosolvents: the simplicity of the complicated*, Adv. Protein Chem. 51 (1998), p. 355.
[96] A.M. Massari et al., *The Influence of aqueous versus glassy solvents on protein dynamics: vibrational echo experiments and molecular dynamics simulations*, J. Am. Chem. Soc. 127 (2005), p. 14279.
[97] R.D. Lins, C.S. Pereira, and P.H. Hünenberger, *Trehalose–protein interaction in aqueous solution*, Proteins-Struct. Funct. Bioinform. 55 (2004), p. 177.
[98] G. Cottone et al., *Molecular dynamics simulation of sucrose- and trehalose-coated carboxy-myoglobin*, Proteins 59 (2005), p. 302.
[99] S.D. Allison et al., *Hydrogen bonding between sugar and protein is responsible for inhibition of dehydration-induced protein unfolding*, Arch. Biochem. Biophys. 365 (1999), p. 289.